Clinical Medicine & Pharmacology



Research article

https://doi.org/10.70731/2h996x12

Serum tsRNA Profile of Nasopharyngeal Carcinoma Patients with Various Chinese Medicine Syndrome

Qi Tang a,b, Yao Wu b, Lin Chen b, Faqing Tang a,b,*

- ^a Hunan Key Laboratory of Oncotarget gene, Hunan Cancer Hospital, and The affiliated Cancer Hospital of Xiangya School of Medicine, Central South University, Changsha 410013, China
- b Department of Clinical Laboratory, Hunan Cancer Hospital, Changsha 410013, China

KEYWORDS

TCM Syndrome Types; Nasopharyngeal Carcinoma; tsRNA; Gene Expression; RNA Sequencing

ABSTRACT

The incidence of nasopharyngeal carcinoma (NPC) is related to genetic factors, and individual genetics determines the physical constitution and syndrome type. The Traditional Chinese Medicine (TCM) studies have proven that NPC patients with different TCM syndrome types should be given various TCM treatment formulas, and the patients get various effects, but the molecular mechanisms are not clear. This study used small RNA microarray sequencing to analyze differential tsRNA of serum samples from NPC patient with TCM syndrome type, and molecular expression profiles in NPC with various CTM syndrome were obtained. 3,718 tsRNAs were highly expressed in NPC patients when compared with healthy population. In the pattern of lung heat with phlegm coagulation, 47 tsRNAs were up-regulated and 11 were down-regulated. Remarkably, tRF3b-ArgACG-2, 5'tiRNA-32-ValAAC-1, mt-tRF3-21-ValTAC, mttRF3-24-ValTAC, and mt-tRF3-20-ValTAC exhibited up-regulation. While 5'tiRNA-36-GlnCTG-6, tRF3b-PheGAA-11, tRF5-18-AsnGTT-15, tRF5-30-GlnTTG-3, 5'tiRNA-35-LeuTAG-1 were down-regulated. In Qi stagnation with phlegm stasis, 16 tsRNAs were up-regulated and 16 tsRNAs were down-regulated. tRF-1-GluCTC-5-1, tRF3b-ArgACG-2, 5'tiRNA-32-ValAAC-2, 5'tiRNA-35-GlnTTG-6, and 5'tiRNA-34-GlnTTG-6 showed up-regulation. tRF5-18-GlnTTG-5, tRF5-18-GluTTC-9, i-tRF-29:51-Asn-GTT-1, tRF5-18-GlyCCC-6, and i-tRF-21i22:46-Lys-CTT-1 were down-regulated. For fire toxin obstruction, 19 tsRNAs were up-regulated and 32 tsR-NAs were down-regulated. mt-tRF3-19-ValTAC, mt-tRF3a-ValTAC, tRF5-22-Val-CAC-6, mt-tRF5-25-TyrGTA, and 5'Leader-ThrAGT-1-1 were upregulated. tRF3b-GluTTC-4, 5'tiRNA-37-LeuAAG-4, 5'Leader-ThrAGT-4-1, mt-tRF3-17-ThrTGT, and 3'tiRNA-45-AlaCGC-4 were down-regulated. The Qi-Yin deficiency group showed 6 upregulated and 1 downregulated tsRNA. i-tRF-15:32-His-GTG-1, mt-tRF5-26-Leu-TAA, 5'tiRNA-37-AsnGTT-7, mt-tRF5-22-MetCAT, tRF5-30-HisGTG-1, and itRF-21:54-His-GTG-1 were upregulated. tRF3a-AlaAGC-10 was down-regulated. Specific tsRNA profiles for each syndrome are revealed, NPC patients with different TCM syndrome types have various tsRNA profile.

^{*} Corresponding author. E-mail address: tangfq@hnca.org.cn

Introduction

In Traditional Chinese Medicine (TCM), nasopharyngeal carcinoma (NPC) is classified as "nasal sinusitis" and "wasting syndrome", and its occurrence is closely associated with deficiency of Zheng Qi (vital energy) and invasion of external pathogens. Through these literatures[1-4], the common TCM syndrome patterns of nasopharyngeal carcinoma are identified as: (1) Lung heat with phlegm accumulation pattern; (2) Qi stagnation with phlegm stasis pattern; (3) Fire toxin obstruction pattern; (4) Qi and Yin deficiency pattern.

NPC is prevalent in southern China and Southeast Asia[5]. There were approximately 120,000 new cases of NPC globally, with about 70,000 deaths, accounting for 0.77% of all cancers[6] [2]. China accounts for over 40% of global cases, with around 60,000 new cases annually, making it one of the most common types of head and neck tumors[7] [3]. The pathogenic factors are relatively complex, and studies have shown that the occurrence and development of nasopharyngeal carcinoma may be the result of the combined effects of genetic factors, environmental factors, EBV (Epstein-Barr Virus) infection, and tsRNA[8,9].

Transfer RNA-derived small RNAs (tsRNAs) are a newly discovered class of functional RNA molecules originating from mature tRNA or precursor tRNA[5]. They are abnormally expressed under various conditions, such as exposure to ultraviolet radiation, treatment with arsenite, heat shock, hypoxia, oxidative damage, or viral infection[6]. These diverse tsRNAs assemble into distinct and stable molecules that participate in multiple biological processes, including the stress response, tumorigenesis, stem cell biology, and epigenetics[7,8]. Growing evidence indicates that tsRNAs play a critical role in human cancers, with great potential as biomarkers for early tumor detection, clinical diagnosis, and prognosis assessment.

This study analyzes differential tsRNA molecular expression profiles in NPC from the perspective of traditional Chinese medicine (TCM) theory. The newly diagnosed NPC patients hospitalized at Hunan Cancer Hospital were enrolled in this study from March to September 2023. The clinical information of the enrolled patients was collected according to diagnostic criteria and inclusion criteria. The indicated serum samples were obtained from NPC patients with different TCM syndromes and healthy controls. The serum samples were subjected to for small RNA microarray sequencing analysis, and tsRNA sequencing data of the serum samples were obtained. By comparing the tsRNA sequencing data among different NPC syndromes, specific tsRNA profiles for each syndrome were revealed.

Methods

Diagnostic Criteria

The medical diagnostic criteria for NPC patients refer to the Chinese Society of Clinical Oncology (CSCO) Guidelines for Diagnosis and Treatment of Nasopharyngeal Carcinoma 2024 [9].

- Principal clinical manifestations: bloody nasal discharge, hearing impairment, nasal congestion, headache, tinnitus, deafness, ear fullness/blockage, double vision, facial numbness.
- 2) **Typical manifestations**: nasopharyngeal tumor, swollen cervical lymph nodes, cranial nerve damage.

- 3) Imaging diagnosis: In nasopharyngeal examinations, non-contrast and contrast-enhanced MRI revealing localized mucosal thickening or invasion of adjacent tissues were suggested malignancy. For primary tumor assessment, non-contrast and contrast-enhanced MRI of the nasopharynx was recommended. Regarding regional lymph node evaluation, non-contrast and contrast-enhanced MRI of the neck was advised. For distant metastasis evaluation, non-contrast and contrast-enhanced CT of the chest, abdominal ultrasound, or non-contrast and contrast-enhanced MRI/CT of the upper abdomen, along with radionuclide bone scan and PET/CT were recommended. Small lymph nodes that yield inconclusive results on MRI but positive on PET/CT should be classified as metastatic.
- 4) Pathological diagnosis: Biopsy through nasopharyngoscopy (using forceps or needle aspiration) confirms nasopharyngeal carcinoma based on tissue pathology. The pathological diagnosis reveals metastatic non-keratinizing carcinoma and metastatic undifferentiated carcinoma by neck mass. For cases with unclear pathology, additional immunohistochemistry or hybridization in situ was necessary to support the pathological diagnosis.

Inclusion Criteria

- 1) Patients were diagnosed as NPC through imaging examination and pathological diagnosis.
- 2) The age ranged from 18 to 80 years old, with no gender limitation.
- Patients newly diagnosed with NPC have not received any treatment.
- 4) Patients with detailed medical records.
- 5) Patients have fully understood and voluntarily signed a written informed consent form for this study.

Exclusion Criteria

- 1) NPC patients not meeting the above inclusion criteria.
- 2) Patients currently undergoing chemotherapy, radiotherapy, targeted therapies, and other immunotherapies.
- 3) Patients with other serious and uncontrolled systemic diseases like cardiovascular, liver, and kidney diseases.
- Individuals who suffer from mental illness, severe cognitive impairment or speech-expression defects and are unable to cooperate.
- 5) Pregnant or lactating women.
- 6) Patients with other malignant tumors.

Standard of TCM Syndrome Types for NPC

The TCM syndrome types related to the diagnosis and treatment of NPC were from various guidelines, textbooks, and books. After consulting three experienced chief physicians and professors, four TCM syndrome types were identified for this study, based on common clinical symptoms: the lung heat-phlegm coagulation type (Chinese abbreviation-PRTN), the qi stagnation-phlegm stasis type (Chinese abbreviation-QYTY), the fire-toxin obstruction type (Chinese abbreviation-HDNZ), and the qi-yin deficiency type (Chinese abbreviation-QYKX). For each syndrome type, serum samples from five patients were selected for subsequent tsRNA microarray sequencing analysis. The clinical observation table is provided in **Supplementary File 1**.

1) Pattern of lung heat with phlegm accumulation: Yellow nasal discharge mixed with blood, occasional coughing, a bitter taste in the mouth, a dry throat, headache, a

- red tongue with a thin yellow coating, and a slippery, rapid pulse.
- 2) Pattern of Qi stagnation with phlegm stasis: nasal obstruction, epistaxis, hearing loss and tinnitus, chest and rib distention and tightness, heavy and distended headache were with a fixed pain site, neck masses, dark red tongue with a thick and greasy coating, slippery or wiry and rapid pulse.
- 3) Pattern of fire toxin obstruction: nasal blockage and epistaxis, thick, yellow and malodorous nasal discharge, severe headache or migraine, double vision or deviated tongue, or facial paralysis (facial distortion), dry mouth with a bitter taste, restlessness and insomnia, constipation, dark-colored urine, a red tongue with a yellow or yellow-ish-greasy coating, and a wiry, rapid pulse.
- 4) Pattern of Qi and Yin deficiency: dizziness and cephalalgia, dry lips and throat, emaciation, dyspnea and asthenia, palpitations and anorexia, numbness in the hands and feet, neck masses, a delicate red or deep red tongue, or with fissures, little or no coating, a thready and rapid pulse.

Serum Samples

From March 2024 to December 2024, the serum samples were collected from 20 newly-diagnosed NPC patients and 5 normal individuals who had undergone routine physical examination at Hunan Cancer Hospital. The normal individuals served as the control group, and the NPC patients were the experimental group. The NPC patients were diagnosed clinically, pathologically, and radiologically. This study was reviewed and approved by the Ethics Committee of the Hunan Cancer Hospital and Institute (No.2024 [30], Supplementary File 2). The blood samples were collected from each participant using 5mL vacuum blood collection tubes without anticoagulant or coagulant. After being left at room temperature for 30 min, the blood samples were first centrifuged at 3000 rpm for 10 min, the supernatant was transferred into a new 1.5 mL EP tube. Then 12000 rpm for 10min at 4°C, again, suck the serum into a new 1.5 mL eppendorf (EP) tube. Serum samples were stored at -80°C for subsequent experiments.

RNA Extraction

According to the manufacturer's instructions, total RNA was isolated using TRIzol Reagent (15596026CN, invitrogen, CA, USA). The quantity of each RNA sample was checked using the Ultramicro biodetector (BIODRPOULIFE, Thermo Scientific, MA, USA), and the integrity of RNA was assessed using agarose gel (2%) electrophoresis. For each sample, a total 100 ng RNA was subjected to dephosphorylation to form a unified 3-OH end. The RNA with 3-OH ends was then denatured using DMSO and enzymatically labeled with Cy3. Subsequently, the Cy3-labeled small RNAs were hybridized to Arraystar Human Small RNAArrays in Agilent Hybridization Oven.

RNA Labeling

In the Small RNA Microarray profiling (5190, Agilent, USA) assay, 100 ng of total RNA was first dephosphorylated with 3 units of T4 polynucleotide kinase (T4PNK) at 37°C for 40 min. This process aimed to eliminate both (P) and (cP) chemical groups from the 3' end of RNA, resulting in the formation of a 3-OH end. The reaction was terminated at

70°C for 5 min and then cooled immediately to 0°C. Subsequently, $7\mu L$ of DMSO was added and the mixture was heated to 100 °C for 3 min to unfold the RNA, followed by immediate chilling to 0 °C. RNA end labeling was performed by adding ligase buffer, BSA, a final concentration of 50 mM pCp-Cy3, and 15 units of T4 RNA ligase in a total volume of 28 μL , and then the reaction mixture was incubated at 16°C overnight.

Array Hybridization

 $22.5\mu L$ 2×Hybridization buffer (G2445A, Agilent, USA) was mixed with the completed labeling reaction solution until the final volume reached 45 μL . The mixture was heated at 100°C for 5 min, then chilled immediately to 0°C. Next, 45 μL labeled sample mix was hybridized onto a microarray at 55°C for 20 h. The slides were washed in 6×SSC containing 0.005% Triton X-102 at room temperature for 10 min, then by immersion in 0.1×SSC with 0.005 % Triton X-102 for 5 min. After the washing process, the slides were scanned on an Agilent G2539A microarray scanner (5188, Agilent, USA).

tsRNA Data Analysis

The scanned microarray images were imported into Agilent Feature Extraction software to extract raw intensity data. The probe signals passing "P" (Present) or "M" (Marginal) QC flags in at least 5 samples were selected for further analysis. Quality normalization was performed using Agilent GeneSpring GX 12.1 software, and the normalized intensities were log₂ transformed. After normalization and signal QC flag filtering, the probe signals for the same small RNA biotype were grouped and analyzed correspondingly. The normalized intensities of multiple probes were averaged for the same small RNA and combined them into an RNA level. To compare two groups in terms of differential small RNA expression, the fold change (FC) was calculated for each small RNA. And the statistical significance of the difference (Pvalue) was also calculated. The default thresholds were set as $FC \ge 1.5$ and P < 0.05. Based on these thresholds, differentially expressed small RNAs were annotated with genomic and biological information, and analyzed through scatter plot, volcano plot and hierarchical clustering heatmap.

Data Visualization Analysis

The samples were grouped through clustering analysis based on the similarities in small RNA expression and the proximity of their relationships, which were shown in the dendrogram above the heatmaps. The expression levels were depicted using a color gradient and visually presented via color scales. The scatter plot plots depicted the normalized intensities of each small RNA in the two samples, which being compared or group-averaged normalized intensities in the two groups. It can be used to visualize, at the abundance levels (normalized intensities), the differentially expressed small RNAs (data point distances off the diagonal lines). For each small RNA comparison between the two groups (each group must have more than 2 replicates), the Volcano plot was constructed by plotting -log10(p) as the differential significance on the Y-axis and log₂ (FC) as the differential magnitude on the X-axis. Thus, small RNAs with large differential significance and large magnitudes (colored in the Volcano plot) were the most likely differentially expressed small RNAs. To determine the potential target genes of the validated tsRNAs, the database of TargetScan (https://www.targetscan.org/vert/) was filtered, and then the target genes were predicted by Miranda (https://www.microrna.org/microrna/).

Results

Tongue Picture Analysis of Different TCM Syndrome Types of NPC

During the clinical case collection, the patients with lung heat with phlegm coagulation pattern were found to be relatively rare. The main tongue presentation included a red or pale-red tongue with a thin coating that was either yellow or white, with yellow being more prevalent. This coating was concentrated mainly at the root of the tongue, which is a typical distribution of phlegm patterns in TCM. The clinical symptoms of these patients often included nasal obstruction, productive cough with yellow sputum, and occasional chest tightness.

This type of qi stagnation with phlegm and blood stasis was commonly seen in clinical diagnosis. The main tongue presentation showed a pale red or red tongue, with pale red being more frequent, and occasionally tooth marks on the sides. The coating was thick and white with a yellow tint, covering the entire tongue, and appearing white and thick with yellow at the root. Its ymptoms typically included nasal congestion, bloody nasal discharge, tinnitus, feeling of fullness in the ears, hearing loss, dry mouth with bitter taste, and commonly present with swollen lymph nodes typically on the affected side of the neck.

In clinical practice, the syndrome of heat-toxin accumulation was extremely uncommon, accounting for the smallest number of cases in the study. The main tongue signs were a dry and red tongue with a thick yellow coating and central fissures, or occasionally a thick white coating with fissures. The patients typically presented with nasal discharge containing blood streaks, nasal congestion and pain, deafness, tinnitus, a feeling of fullness or blockage in the ears, and hearing loss. Other symptoms included headache, facial numbness, and diplopia (double vision). On the affected side of the neck, the mass typically shows redness, swelling, and pain, and might ulcerate occasionally.

The Qi-Yin deficiency pattern was the most common observed in clinical practice. Due to the metabolic burden imposed by the tumor and chronic Qi stagnation, the patients often experienced involuntary weight loss, severe fatigue,

and exhaustion, which in turn led to the internal depletion of body fluids. The main tongue manifestations included a palered tongue with scalloped edges and a thin white coating, sometimes moist or slippery. The symptoms included nasal congestion, tinnitus, and progressive hearing loss, without other major accompanying symptoms.

tsRNA Difference in Lung Heat With Phlegm Accumulation Type

Following the processing and analysis of the tsRNA chip data, 3,718 tsRNAs were detected in serum samples form NPC patients when compared with the healthy group. In the pattern of lung heat with phlegm coagulation, 47 tsRNAs were up-regulated and 11 were down-regulated, remarkably, tRF3b-ArgACG-2, 5'tiRNA-32-ValAAC-1, mt-tRF3-21-ValTAC, mt-tRF3-24-ValTAC, and mt-tRF3-20-ValTAC exhibited significant up-regulation. The top 10 expressions are shown in **Table 1**. While 5'tiRNA-36-GlnCTG-6, tRF3b-PheGAA-11, tRF5-18-AsnGTT-15, tRF5-30-GlnTTG-3, 5'tiRNA-35-LeuTAG-1 were significantly down-regulated. **Table 2** lists the top 10 expressions. **Figure 1** presents the volcano plot and cluster analysis heatmap of these differentially expressed tsRNAs.

tsRNA Difference in Qi Stagnation With Phlegm Stasis Type

16 tsRNAs were up-regulated and 16 tsRNAs were down-regulated in the pattern of Qi stagnation with phlegm stasis when compared to the healthy group, . Significantly, tRF-1-GluCTC-5-1, tRF3b-ArgACG-2, 5'tiRNA-32-ValAAC-2, 5'tiRNA-35-GlnTTG-6, and 5'tiRNA-34-GlnTTG-6 showed remarkable up-regulation. The top 10 expressions are listed in **Table 3**. Meanwhile, tRF5-18-GlnTTG-5, tRF5-18-GluTTC-9, i-tRF-29:51-Asn-GTT-1, tRF5-18-GlyCCC-6, and i-tRF-21i22:46-Lys-CTT-1 were significantly down-regulated. The top 10 expressions are listed in **Table 4**. The volcano plot and the cluster analysis heatmap of the differentially expressed tsRNAs are presented in **Figure 2**.

tsRNA Difference in Fire Toxin Obstruction Type

Compared to the healthy group, 19 tsRNAs were up-regulated and 32 tsRNAs were down-regulated in the pattern of fire toxin obstruction. Notably, mt-tRF3-19-ValTAC, mt-tR-F3a-ValTAC, tRF5-22-ValCAC-6, mt-tRF5-25-TyrGTA, and

tsRNA-name	NA-name Fold Change		FDR	FRTN (mean)	Control (mean)
tRF3b-ArgACG-2	3.653195446	0.000277693	0.25950395	4.25811364	2.3889547
5'tiRNA-32-ValAAC-1	3.605291523	0.036490754	0.646323018	6.06739152	4.2172756
mt-tRF3-21-ValTAC	3.257151841	0.023445299	0.642843457	5.273850618	3.570239642
mt-tRF3-24-ValTAC	3.222424693	0.029698011	0.646323018	5.656005421	3.967858777
mt-tRF3-20-ValTAC	3.143658974	0.019303457	0.629428693	4.953533725	3.301089004
tRF3a-ArgACG-1	3.128253355	0.021731389	0.629428693	4.10529632	2.45993896
mt-tRF3-19-ValTAC	3.117514567	0.010235348	0.5626411	4.553124014	2.912727712
mt-tRF3b-ValTAC	2.951736946	0.043144279	0.646323018	5.380255708	3.818691551
mt-tRF3-17-ValTAC	2.898212709	0.007394818	0.5626411	4.492982809	2.957819326
mt-tRF3a-ValTAC	2.853634298	0.011480041	0.5626411	4.333468173	2.820667713

Table 2 | Downregulated tsRNAs of lung heat with phlegm coagulation type

tsRNA-name	Fold Change	<i>P</i> -value	FDR	FRTN(mean)	Control(mean)
5'tiRNA-36-GInCTG-6	0.66456219	0.039864635	0.646323018	3.78347096	4.37299484
tRF3b-PheGAA-11	0.657459012	0.026674376	0.646323018	2.4694537	3.07448084
tRF5-18-AsnGTT-15	0.656565514	0.003410526	0.502966637	4.27445488	4.881444
tRF5-30-GInTTG-3	0.64903336	0.003265235	0.502966637	3.20379032	3.82742578
5'tiRNA-35-LeuTAG-1	0.646896387	0.024972927	0.643784828	3.88812944	4.51652288
i-tRF-52:70-Glu-CTC-1	0.644442274	0.000750849	0.350833982	2.7003382	3.33421516
5'tiRNA-36-GInCTG-4	0.633512794	0.031282413	0.646323018	2.65799408	3.31654842
i-tRF-3:31-His-GTG-1	0.632889439	0.006957152	0.5626411	2.86530982	3.52528442
tRF-1-GInTTG-4-1	0.615474231	0.034602338	0.646323018	3.66345712	4.36368676
i-tRF-16:31-Arg-TCT-1	0.564099858	0.013261272	0.5626411	3.9431096	4.76908712

Table 3 | Upregulated tsRNAs of Qi stagnation with phlegm stasis type

tsRNA-name	Fold Change	<i>P</i> -value	FDR	QYTY (mean)	Control (mean)
tRF-1-GluCTC-5-1	2.992536077	0.025463009	0.853054078	5.4237078	3.84233916
tRF3b-ArgACG-2	1.906811062	0.039254257	0.8602812	3.3201166	2.3889547
5'tiRNA-32-ValAAC-2	1.865452209	0.014295302	0.853054078	4.21804652	3.31852112
5'tiRNA-35-GInTTG-6	1.811659139	0.005046793	0.765194762	6.71517154	5.85786
5'tiRNA-34-GInTTG-6	1.788334362	0.004841925	0.765194762	6.67322306	5.83460656
mt-tRF5-26-LeuTAA	1.745582738	0.00592065	0.765194762	3.62547078	2.82176204
tRF5-31-HisGTG-1	1.694888327	0.046700559	0.8602812	5.87015436	5.10896414
tRF3a-ProTGG-5	1.64042314	0.043295819	0.8602812	3.5076191	2.7935511
tRF-1-GlnCTG-4-1	1.599177656	0.023748371	0.853054078	5.62983162	4.9525014
5'tiRNA-29-GlyCCC-7	1.592643227	0.022036054	0.853054078	3.39883284	2.72740972

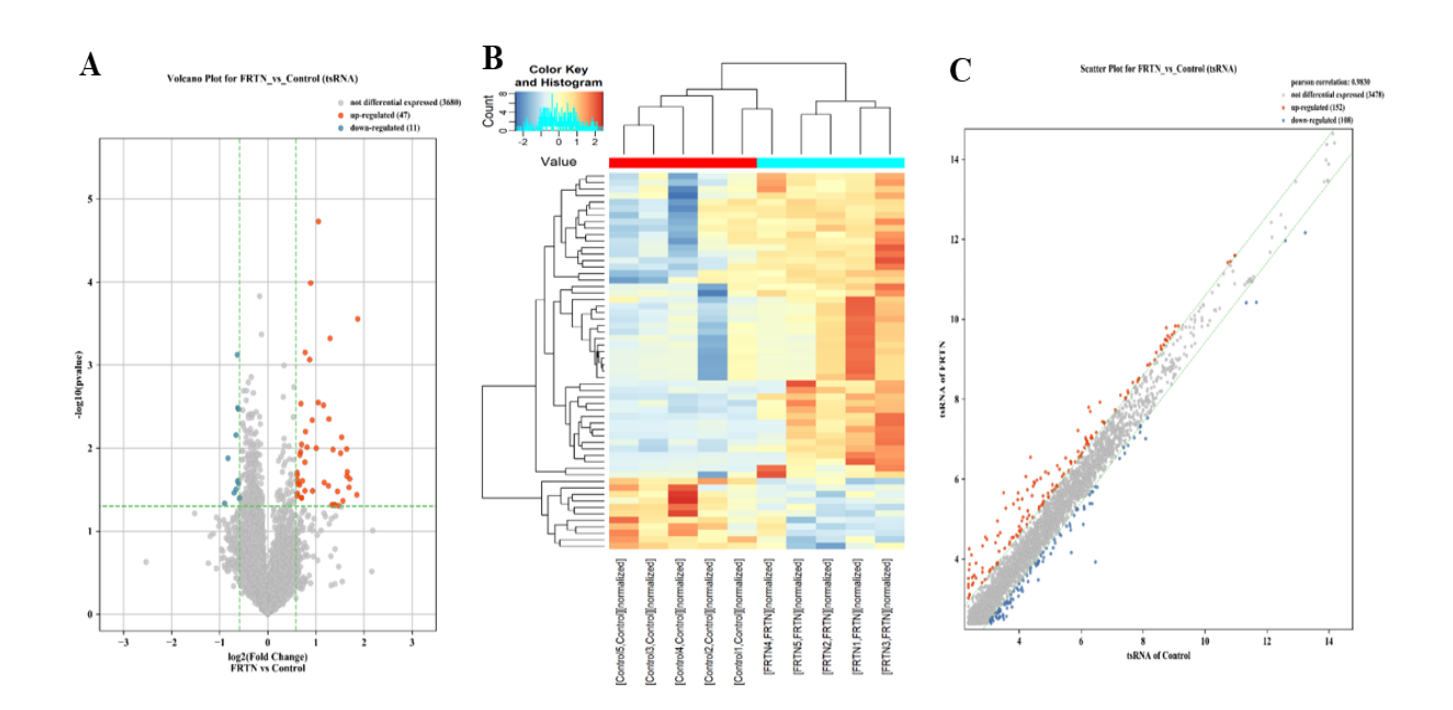


Figure 1 | Visualization diagram of differential tsRNA between the lung heat with phlegm coagulation type and the healthy group. A, Volcano plot; B, Hierarchical clustering heatmap; C, Scatter plot.

Table 4 | Downregulated tsRNAs of Qi stagnation with phlegm stasis type

tsRNA-name	Fold Change	<i>P</i> -value	FDR	QYTY (mean)	Control (mean)
tRF5-18-GInTTG-5	0.664276757	0.02498036	0.853054078	3.76232214	4.3524658
tRF5-18-GluTTC-9	0.664216396	0.021612749	0.853054078	5.18947604	5.7797508
i-tRF-29:51-Asn-GTT-1	0.659281197	0.029457889	0.853054078	2.97923308	3.58026724
tRF5-18-GlyCCC-6	0.65901295	0.011636599	0.81274002	5.1383296	5.73995088
i-tRF-21i22:46-Lys-CTT-1	0.656833466	0.002564005	0.765194762	4.29442668	4.90082714
i-tRF-11:30-Gln-CTG-1	0.651607755	0.003622314	0.765194762	2.73228622	3.35021054
tRF5-18-SerAGA-1	0.648870769	0.000556216	0.521833875	4.43832278	5.0623197
tRF5-18-MetCAT-2	0.646919058	0.032139794	0.853054078	3.12791018	3.75625306
tRF5-18-AspGTC-4	0.63934248	0.005943569	0.765194762	4.35769616	5.0030353
5'Leader-AspGTC-2-8	0.637864706	0.032177802	0.853054078	2.72576736	3.374445

Table 5 | Upregulated tsRNAs of Fire toxin obstruction type

tsRNA-name	Fold Change	<i>P</i> -value	FDR	HDNZ(mean)	Control(mean)
mt-tRF3-19-ValTAC	2.895598322	0.037656102	0.56361813	4.446589198	2.912727712
mt-tRF3a-VaITAC	2.66331685	0.0372177	0.56361813	4.233891786	2.820667713
tRF5-22-ValCAC-6	1.714686822	0.040045663	0.56361813	6.69765904	5.91971394
mt-tRF5-25-TyrGTA	1.681110271	0.045772304	0.56361813	5.58600056	4.8365862
5'Leader-ThrAGT-1-1	1.632894316	0.017645458	0.56361813	3.46168486	2.75425344
tRF3b-LysTTT-10	1.611263225	0.022863905	0.56361813	3.66754504	2.97935284
mt-tRF5-24-TyrGTA	1.590518332	0.046920081	0.56361813	5.95464006	5.28514306
tRF5-22-ValCAC-13	1.586950645	0.015161456	0.56361813	3.64644088	2.98018362
5'tiRNA-36-ArgCCG-1	1.58661791	0.041870115	0.56361813	3.3417669	2.67581216
i-tRF-38:57-Phe-GAA-1	1.580029659	0.015320365	0.56361813	4.77984808	4.11989644

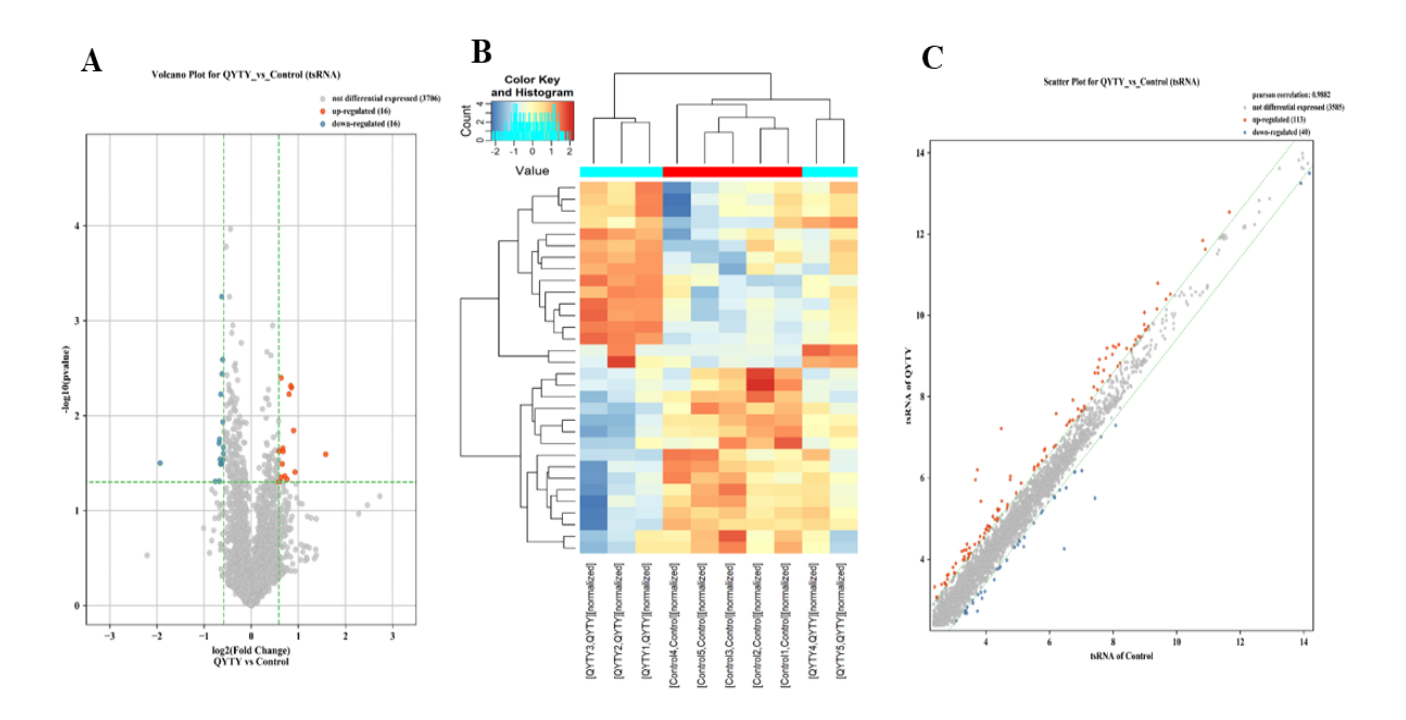


Figure 2 | Visualization diagram of differential tsRNA between the Qi stagnation with phlegm stasis type and the healthy control group. A, Volcano plot; B, Hierarchical clustering heatmap; C, Scatter plot.

3.53270288

4.0861287

tsRNA-name	Fold Change	<i>P</i> -value	FDR	HDNZ (mean)	Control (mean)
tRF3b-GluTTC-4	0.661155908	0.012827118	0.56361813	2.80711	3.40404758
5'tiRNA-37-LeuAAG-4	0.658564961	0.048087601	0.56361813	3.52814634	4.13074868
5'Leader-ThrAGT-4-1	0.652981851	0.03512111	0.56361813	5.07410458	5.68898978
mt-tRF3-17-ThrTGT	0.649315647	0.017800907	0.56361813	4.21173494	4.83474306
3'tiRNA-45-AlaCGC-4	0.644722126	0.006756744	0.56361813	4.35725036	4.99050096
i-tRF-12:33-Lys-CTT-1	0.643156866	0.049937332	0.56361813	7.6109205	8.24767794
i-tRF-20:39-Gly-GCC-1	0.641417775	0.03600109	0.56361813	2.45894232	3.09960608
tRF5-26-ArgCCG-2	0.636742497	0.017821925	0.56361813	3.25132004	3.90253808

0.008308176

0.02790562

0.56361813

0.56361813

Table 6 | Downregulated tsRNAs of Fire toxin obstruction type

0.633856918

0.628606528

3'tiRNA-41-AlaAGC-22

tRF3-20-ThrAGT-5

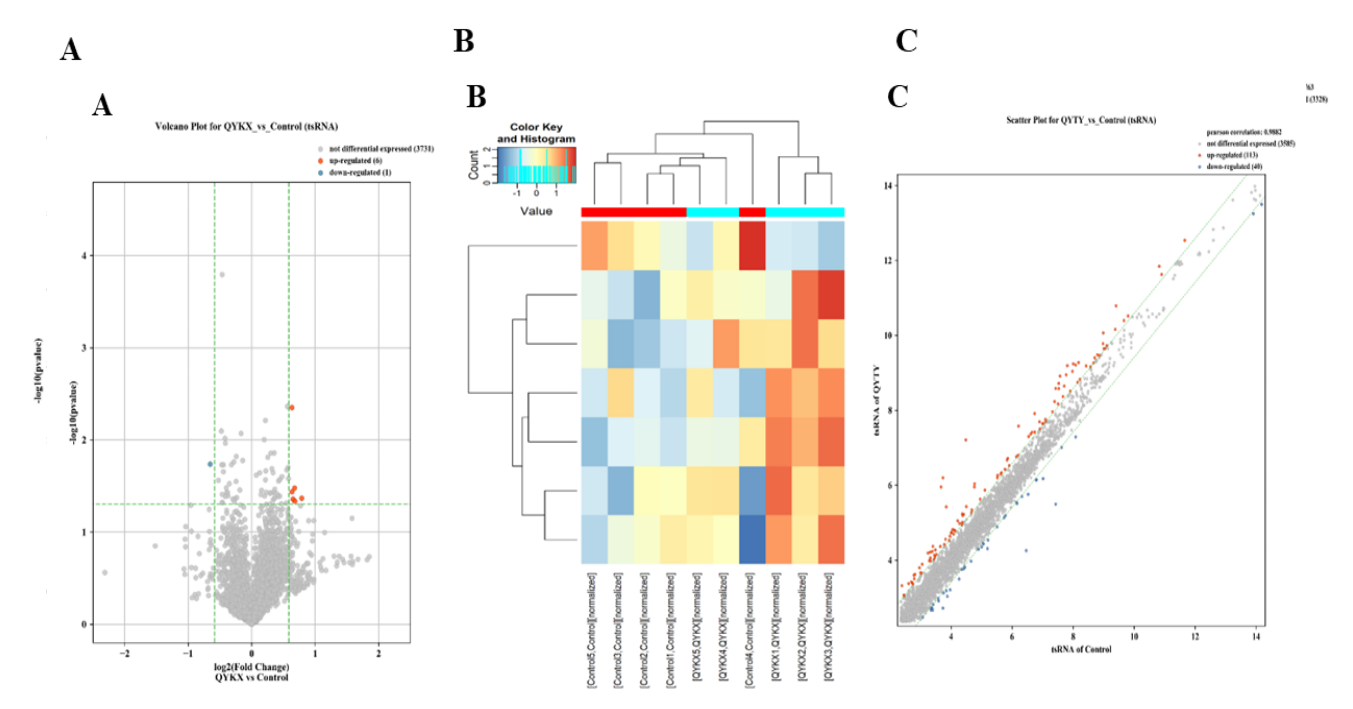


Figure 3 | Visualization diagram of differential tsRNA between the fire toxin obstruction type and the healthy group. A, Volcano plot; B, Hierarchical clustering heatmap; C, Scatter plot.

5'Leader-ThrAGT-1-1 were significantly upregulated. The top 10 expressions are listed in **Table 5**. On the other hand, tRF3b-GluTTC-4, 5'tiRNA-37-LeuAAG-4, 5'Leader-Thr-AGT-4-1, mt-tRF3-17-ThrTGT, and 3'tiRNA-45-AlaCGC-4 were significantly down-regulated. The top 10 expressions are listed in **Table 6**. The volcano plot and the cluster analysis heatmap of the differentially expressed tsRNAs are shown in **Figure 3**.

tsRNA Difference in Qi and Yin Deficiency Type

The Qi-Yin deficiency group showed 6 upregulated and 1 downregulated tsRNA when compared with the healthy group. Specifically, i-tRF-15:32-His-GTG-1, mt-tRF5-26-LeuTAA, 5'tiRNA-37-AsnGTT-7, mt-tRF5-22-MetCAT, tRF5-30-HisGTG-1, and i-tRF-21:54-His-GTG-1 were significantly upregulated, referring to **Table 7** for the tsRNA expression levels. In contrast, tRF3a-AlaAGC-10 was significantly down-regulated, their expression status is shown in

Table 8. Figure 4 presents volcano plots and clustering heatmaps of these differential tsRNAs.

2.874932

3.41635786

Discussion

In this study, four common TCM syndrome patterns of NPC patients were collected and analyzed. Newly diagnosed NPC patients were categorized according to their primary clinical symptoms and characteristic tongue presentations. Under the guidance of senior physicians, the collected cases were classified and analyzed. The following outlines the clinical features of each syndrome pattern and relevant research findings.

The main symptoms of lung heat with phlegm accumulation type include nasal congestion, yellow nasal discharge with blood, occasional coughing, a bitter taste in the mouth, a dry throat, headache, a red tongue with a thin yellow coating, and a slippery and rapid pulse. When external wind-heat

Table 7 | Significantly upregulated tsRNAs in Qi and Yin deficiency type

tsRNA-name	Fold Change	<i>P</i> -value	FDR	QYKX (mean)	Control (mean)
i-tRF-15:32-His-GTG-1	1.72684405	0.042995551	0.999886854	4.2733664	3.4852286
mt-tRF5-26-LeuTAA	1.602077301	0.046196923	0.999886854	3.5017058	2.82176204
5'tiRNA-37-AsnGTT-7	1.596638362	0.033332819	0.999886854	3.43155536	2.75651778
mt-tRF5-22-MetCAT	1.569959562	0.044056686	0.999886854	4.46899286	3.81826546
tRF5-30-HisGTG-1	1.553093601	0.036662226	0.999886854	6.40065468	5.7655099
i-tRF-21:54-His-GTG-1	1.551716715	0.004456551	0.999886854	3.57072866	2.93686346

Table 8 | Downregulated tsRNAs of Qi and Yin deficiency type

tsRNA-name	tsRNA-name Fold Change		FDR	QYKX(mean)	Control(mean)
tRF3a-AlaAGC-10	0.635388137	0.018297956	0.999886854	4.22654148	4.88083142

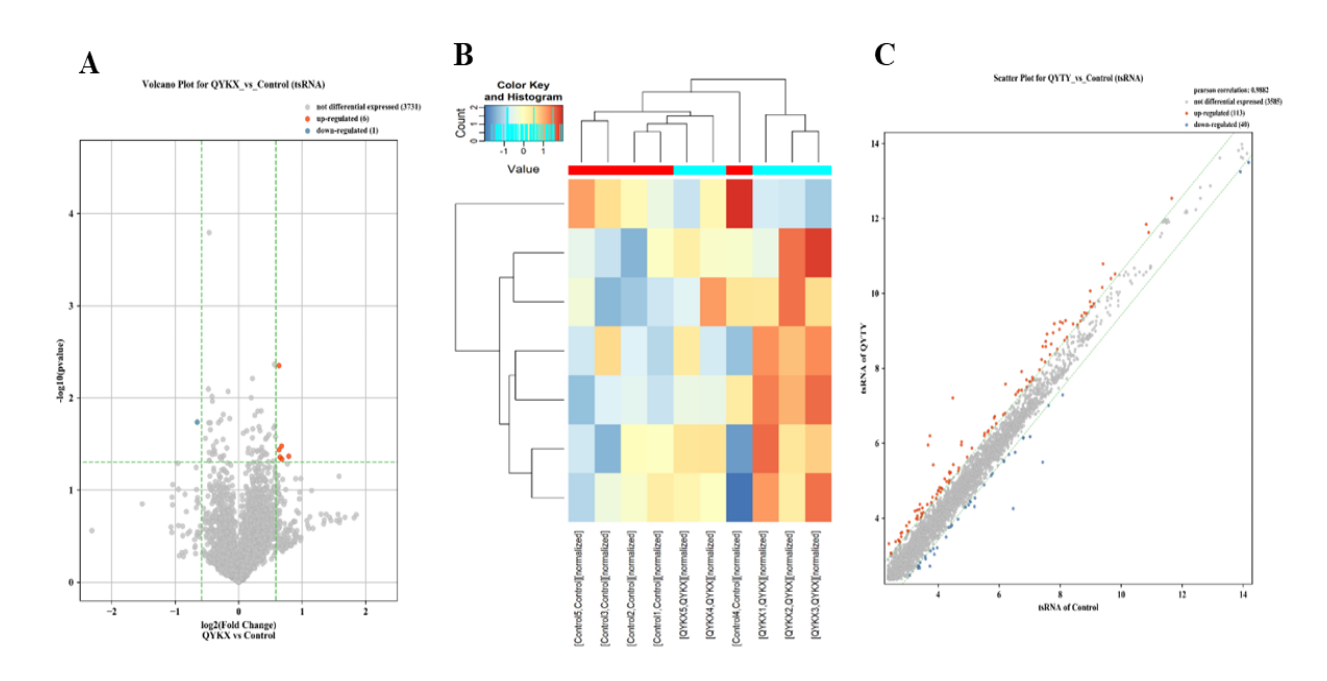


Figure 4 | Visualization diagram of differential tsRNA between the Qi and Yin deficiency type and the healthy group. A, Volcano plot; B, Hierarchical clustering heatmap; C, Scatter plot.

pathogens invade the nose, the qi flow is obstructed, resulting in nasal congestion. Intense heat in the lungs causes the lung qi to rebel, leading to coughing. Heat transforms body fluids into phlegm and damages blood vessels, causing yellow nasal discharge with blood. Heat toxins deplete vin fluids, resulting in a bitter taste and a dry throat. Heat pathogens disrupt clear orifices (sensory organs), causing headache. A red tongue with a thin yellow coating and a slippery and rapid pulse are manifestations of internal phlegm-heat obstruction. During clinical case collection, the researchers discovered that there are relatively few patients with the lung heat and phlegm congestion type. The main tongue appearances are a red or light-red tongue with a thin vellow or thin white coating, mostly thin yellow and mainly concentrated at the back of the tongue. The patients usually present with nasal congestion, coughing with abundant yellow phlegm, and occasional chest tightness.

Xiong D believed[10] that the lungs open onto the nose, being a delicate organ, they are prone to invasion by external pathogens, leading to illness. Due to the perennial hot and humid climate in the Lingnan region and the coastal location where people enjoy eating raw and cold foods, such as seafood, the patients often have an internal accumulation of damp-heat pathogens. Consequently, when the body is exposed to external pathogens, they can stagnate and transform into heat, ascending to invade the nasal passages, resulting in the pattern of latent heat in the lung meridian. Excessive lung heat often damages the blood vessels, forcing blood to move recklessly, leading to epistaxis. Treatise on Causes and Manifestations of Various Diseases states: "The lungs open onto the nose, when heat invades the blood, the qi also becomes hot. When both blood and qi are hot, blood is driven by qi and emerges from the nose, causing epistaxis." The pathogenesis involves the six external pathogens invading the body, with the nose being the first affected. The pathogens

enter the lung-defense system, compromising the defensive Oi, and penetrate deeper, transforming into heat along the meridians. This forces blood to move recklessly, scorching the nasal collaterals and causing blood to spill outside the vessels, and finally resulting in epistaxis[11]. Another clinical symptom of lung-heat-type NPC patients is runny nose. The nose serves as the orifice of the lungs. When lung heat is extreme, it forces fluids outward through the nose to drain the lung heat. Extreme lung heat steams fluids, forcing them out as clear nasal discharge[12]. When lung heat stagnates in the nasal passages, it causes itching. While the steaming of lung qi overflows the nasal passages, leading to a continuous flow of clear discharge. When lung qi becomes impaired, the ancestral qi becomes obstructed, resulting in nasal congestion[13]. Therefore, the lung-heat-phlegm-coagulation pattern is a well-founded pattern in TCM differentiation for NPC and serves as a valuable reference pattern in clinical practice.

The main symptoms of Qi stagnation with phlegm stasis include nasal congestion, epistaxis (nosebleeds), hearing impairment, tinnitus, distension and tightness in the chest and ribs, heavy distending headache with fixed pain locations, neck masses, dark red tongue with thick greasy coating, and slippery or wiry rapid pulse. The liver governs the free flow of qi and regulates both qi movement and emotional states. Emotional distress or external pathogens invading the liver meridian can impair its dredging function, leading to liver qi stagnation, which manifests as chest and rib distension, tightness, and distending headache. Blocking qi movement hinders blood circulation and fluid distribution, eventually resulting in blood stasis and phlegm coagulation, which presents as fixed pain locations and neck masses. Blood stasis obstructing collaterals causes blood to escape vessels, leading to epistaxis. Liver qi stagnation disrupts qi and blood flow, depriving the ears of nourishment and resulting in hearing impairment and tinnitus. A dark tongue with thick, greasy coating and a slippery or wiry, rapid pulse indicate internal obstruction by phlegm and blood stasis. This pattern is commonly observed in clinical practice. The primary tongue manifestations include a pale red or red tongue (pale red being more frequent), occasionally with tooth marks on the edges, a white thick coating with yellow tinge covering the entire tongue, particularly thick and white at the root. The patients typically present with nasal congestion, blood-streaked nasal discharge, tinnitus, ear blockage, hearing loss, dry mouth and bitter taste, and frequent lymph node enlargement on the affected side of the neck.

Some scholars considered impaired liver qi dispersion and qi stagnation as a central to the tumor pathogenesis[14]. The Huangdi Neijing proposed the concept that "all diseases arise from Oi," emphasizing the role of emotional factors in causing disease. Based on this, later physicians developed clinical approaches emphasizing emotional regulation as a therapeutic strategy[15]. The seven emotions correspond to the Zangfu organs, and Qing Dynasty physicians noted that "disorders of the seven emotions always start with the liver"[16]. The liver regulates qi circulation, and dysfunction in this role can lead to emotional changes. In internal damage disorders, the internal organs are often affected, with the liver being the first to respond. Therefore, emotional disturbances are often treated by regulating the liver's dispersing function and qi movement[17]. Qi stagnation hinders the flow of fluids and blood, leading to fluid retention and blood stasis. Over time,

this causes pathological products including phlegm turbidity. dampness, and blood stasis. If these persisted, they might eventually form accumulations and cancerous toxins[18]. These pathological products further exacerbate tumor development as causative factors of cancerous toxins, creating a vicious cycle where they fluctuate and interact, mutually reinforcing and challenging to treat. NPC patients experience significant psychological distress, with emotions such as worry, anxiety, fear, depression, or anger. Due to the disease itself, surgery, radiotherapy, chemotherapy, treatment-related suffering, or the financial burden of prolonged treatment, patients' emotional state undergoes corresponding changes. All seven emotions can affect the liver, leading to impaired qi dispersion, gi stagnation, fluid retention, and gi stagnation with blood stasis, ultimately resulting in phlegm aggregation and blood stasis[19]. This study found that the pattern of gi stagnation with phlegm and blood stasis is common among newly diagnosed NPC patients. Other studies have indicated that liver stagnation with phlegm obstruction is the most frequent pattern in newly diagnosed NPC patients[20], which is consistent with the present findings. Therefore, the pattern of qi stagnation with phlegm and blood stasis is supported by TCM pattern differentiation for NPC and should be considered a reference pattern in clinical practice for NPC treatment.

The main symptoms of fire toxin obstruction include nasal congestion and epistaxis, thick yellowish foul-smelling nasal mucus, severe headache or migraine, diplopia and tongue deviation, or facial paralysis, dry mouth with bitter taste, restless insomnia, constipation, deep yellow urine, red tongue with a yellow or yellow-greasy coating, and wiryrapid pulse. When toxic heat affects the qi phase, it manifests as dry mouth with bitter taste. When fire-toxin invades the nutritive and blood levels, consuming blood and causing reckless bleeding, it leads to epistaxis; when heat-toxin stagnates and scorches the nasopharynx, causing tissue putrefaction, it results in thick yellowish foul-smelling nasal mucus; when heat accumulates in the intestines, scorching yin fluids, it causes constipation; when heat-toxin descends to the bladder, it leads to deep yellow urine; when excessive heat-toxin scorches fluids into phlegm, stirring internal wind (windyang), and wind-phlegm ascends, it causes severe headache, even diplopia and tongue deviation, or facial paralysis. A red tongue with yellow-greasy coating and wiry-rapid pulse are all signs of internal obstruction of fire-toxin. The fire-toxin internal obstruction pattern is extremely rare in clinical practice, being the least frequently observed type in case collections. The main tongue manifestations include a red tongue with scanty fluids, yellow thick coating with central cracks, and occasionally white thick coating with cracks. The patient clinical symptoms often include nasal discharge streaked with blood, nasal congestion and pain, deafness with tinnitus, ear fullness and blockage, hearing loss, headache, facial numbness, diplopia, and commonly observed painful red swollen neck masses on the affected side, which may occasionally ulcerate.

The occurrence of NPC results from depletion of healthy Qi, invasion of noxious pathogens, and their stagnation in the nasopharynx. Over time, stagnant pathogens turn into fire, generate phlegm, and lead to blood stasis. As described in *The Orthodox Lineage of External Medicine* (Wai Ke Zheng Zong), NPC is "congealed from depressed fire, with phlegm losing its proper pathway, accumulating and forming" [21].

The patients with internal obstruction by fire-toxin pattern most commonly present with nasal discharge tinged with blood (epistaxis). Ming Dynasty physician Li Chan's Introduction to Medicine (Yi Xue Ru Men) states: "Blood, derived from food essence, is governed by the spleen, heart, liver, and lungs. When it rises abnormally, it exits the nose as epistaxis." Most medical scholars attribute epistaxis primarily to heat and fire [22], as Tang Dynasty's Wang Tao noted in Arcane Essentials from the Imperial Library (Wai Tai Mi Yao): "Epistaxis results from accumulated heat in the five zang organs." Thus, excessive fire-heat rising and yang heat hyperactivity constitute the main pathogenesis of epistaxis[23]. The liver governs ascending movement while the lungs govern descending purification. The mutual regulation maintains the balance of gi dynamics. Conversely, when liver fire surges upward (wood overacting on metal), it damages lung collaterals. As blood vessels rupture, fire drives blood upward to overflow from the nasal passages, causing epistaxis[24]. This liver fire counteracting the lungs represents progression from the earlier qi stagnation with phlegmstasis pattern. Qi-level heat becomes interior lung heat, consuming fluids to form phlegm. As lung disease affects the liver, the condition worsens into liver fire ascending to counteract the lungs, marking NPC's progression. A study that probed correlations between TCM patterns and intracranial invasion potential in newly diagnosed NPC patients identified 12 cases (20%) of fire-toxin accumulation pattern[25]. Another prospective study of 176 cases demonstrated a great neutrophil infiltration in tumor stroma of fire-toxin accumulation patients[26]. Therefore, the internal obstruction by firetoxin pattern has diagnostic validity in NPC and clinical rele-

The main symptoms of Qi and Yin Deficiency include dizziness, headache, dry lips and throat, emaciation, shortness of breath, fatigue, palpitations, poor appetite, numbness in hands and feet, and neck masses. The tongue appears tender red or deep red, sometimes with cracks. The pulse is thready and rapid. When vital qi is deficient and internal organs are weak, the symptoms appear shortness of breath, fatigue, palpitations, and poor appetite manifest. Qi deficiency causes failure of clear yang to ascend, resulting in inadequate nourishment of head and sensory orifices, which hence dizziness, headache, dry lips and throat. Qi deficiency and fluid depletion deprive a body of nourishment, leading to emaciation and numbness in hands and feet. The prolonged internal exuberance of heat toxin scorches fluids into phlegm, which accumulates in the neck, forming masses. Deep red tongue with cracks and no coating, along with thready rapid pulse, are signs of qi and yin deficiency. These patterns are most commonly observed in clinical diagnosis. The patients often experience weight loss and persistent fatigue due to tumor consumption, long-term qi stagnation, and internal depletion of fluids. The primary tongue signs include pale red tongue with scalloped edges (tooth marks) and thin white coating, occasionally with moist, glossy coating. The patients may experience nasal obstruction, tinnitus, and hearing decline, without other notable symptoms.

The interaction of endogenous toxins with external invading toxins, where internal and external pathogens combine to cause illness, forms the pathological basis for the susceptibility of individuals with qi-deficient constitution to toxic pathogens[27]. Tian D's therapeutic formula to NPC with Qi and Yin deficiency pattern is to focus on boosting Qi, nour-

ishing Oin, and supporting healthy energy while dispelling pathogen[28]. Recent studies show that the modified Yiqiyangyin Detoxification not only improves clinical symptoms, physical signs, and inflammation in NPC patients with qi and yin deficiency syndrome, but also reduces oral mucosa damage and adverse reactions[29]. During chemoradiotherapy for NPC, logistic regression analysis of qi and yin deficiency syndrome[30] revealed that, key contributing factors includes dry mouth and thirst, shortness of breath and reluctance to speak, tidal fever and night sweats, five-center heat (heat sensation in palms, soles, and chest), soreness and weakness of waist and knees, hunger without desire to eat, wiry pulse, reduced saliva, and scant or absent tongue coat. The modified Maimendong decoction to the locally advanced NPC with gi and yin deficiency syndrome may improve short-term efficacy, reduce TCM pattern symptoms, improve quality of life, and lessen toxic side effects[31]. The modified Bazhen decoction combined with Antiphlogistic Decoction of Five Drugs can effectively improve the efficacy and symptoms of advanced NPC with qi and yin deficiency syndrome, reduce immune function damage, and decrease adverse reactions[32]. Yangyinquyu decoction demonstrates good efficacy in treating NPC patients with qi and yin deficiency syndrome, and can reduce post-treatment adverse reactions[33]. For advanced EGFR-positive NPC patients with gi and yin deficiency syndrome, the addition of modified Shengmai decoction to nimotuzumab and radiotherapy yields a better clinical treatment efficacy[34]. Yangyinjiedu decoction demonstrates a significant efficacy in advanced NPC patients with qi and yin deficiency syndrome, significantly reducing adverse reactions, immune function damage, and the related fatigue caused by chemoradiotherapy[35]. Therefore, the qi and yin deficiency syndrome, as a pattern of NPC in TCM diagnosis, has an evidence basis and warrants consideration in clinical practice for NPC.

There are currently only two reports on tsRNA targets related to NPC pathogenesis, the reports showed that tRF-1:28-ValCAC-2 and tRF-1:24-Ser-CGA-1-M3 were upregulated, while tRF-55:76-Arg-ACG-1M2 was downregulated in NPC patients[36]. Another study reported NPC cells exhibited tRF-1:28-Val-CAC-2 upregulation that was associated with significantly increased proliferative, migratory, and invasive activity together with the suppression of apoptotic death[37].

Conclusion

In this study, baseline clinical data were collected from newly diagnosed nasopharyngeal carcinoma patients, and Traditional Chinese Medicine pattern differentiation was carried out under the guidance of senior physicians. Based on medical guidelines and literature, it was determined that NPC patients presented four distinct TCM syndrome types: (1) Lung heat with phlegm accumulation type; (2) Qi stagnation with phlegm stasis type; (3) Fire toxin obstruction type; (4) Qi and Yin deficiency type. Serum samples were collected from patients with different syndrome types for Small RNA microarray sequencing, which led to the acquisition of the tsRNA profiles of various TCM syndrome types in NPC, and distinct tsRNA patterns across different TCM syndrome types were identified.

Acknowledgement We thank Professor Qianjin Liao in Medical Research Center of Hunan Hospital and Xiangya Medical School University for contributions

Funding This work was supported in part by the National Science and Technology Major Special Sub-project (2024ZD0521301), the Major Science and Technological Innovation Project of Hunan Province (2025JJ50568, 2021SK1020-4), and the Pandeng Project of Hunan Cancer Hospital (YF2020001).

Ethics statement This study was reviewed and approved by the Ethics Committee of the Hunan Cancer Hospital and Institute (No.2024 [30].

Author contributions Tang Q performed the experiments. Tang Q performed bioinformatic analyses of sequence data. Tang Q prepared all the figures and wrote the manuscript. Tang F supervised the project and revised the manuscript. Tang Q, Wu Y, Chen L, and Tang F convinced whole project. All authors read and approved the final manuscript.

Conflict of interest statement The authors declare no competing financial interests.

Data accessibility statement The datasets generated and analyzed during the current study are available from the corresponding author on reasonable request.

References

- Chinese Society of Traditional Chinese Medicine. Guidelines for Diagnosis and Treatment of Tumor in Traditional Chinese Medicine. Beijing: China Traditional Chinese Medicine Press, 2008:2-3.
- Zhou Daihan. Oncology of Traditional Chinese Medicine. Guangzhou: Guangdong Higher Education Press, 2020:191-202.
- Lang JY, Hu CS, Ma J, et al. China Integrated Guidelines for Diagnosis and Treatment of Nasopharyngeal Carcinoma 2022. Tianjin: Tianjin Science and Technology Press, 2022.05.
- ence and Technology Press, 2022.05.
 Tian DF, Li YY. Otolaryngology of Integrated Traditional Chinese and Western Medicine. Beijing: China Traditional Chinese Medicine Press, 2016:317-324.
- Song YX, Liu XJ, Zhang YQ, et al. Analysis and prediction of nasopharyngeal carcinoma burden in China from 1990 to 2050 based on GBD database. Journal of Central South University (Medical Edition), 1 -9[2025-09-1 - 9].
- Filho AM, Laversanne M, Ferlay J, et al. The GLOBOCAN 2022 cancer estimates: Data sources, methods, and a snapshot of the cancer burden worldwide. Int J Cancer, 2025,156(7):1336-1346.
- Han B, Zheng R, Zeng H, et al. Cancer incidence and mortality in China, 2022. J Natl Cancer Cent, 2024,4(1):47-53.
- Yu KJ, Hsu WL, Chiang CJ, et al. Cancer patterns in nasopharyngeal carcinoma multiplex families over 15 years. Cancer, 2021,127(22):4171-4176.
- Yu WM, Hussain SS. Incidence of nasopharyngeal carcinoma in Chinese immigrants, compared with Chinese in China and South East Asia: review. J Laryngol Otol, 2009,123(10):1067-1074.
- Lu Z, Su K, Wang X, et al. Expression Profiles of tRNA-Derived Small RNAs and Their Potential Roles in Primary Nasopharyngeal Carcinoma. Front Mol Biosci. 2021; 8:780621.
- Chen Q, Li D, Jiang L, et al. Biological functions and clinical significance of tRNA-derived small fragment (tsRNA) in tumors: Current state and future perspectives. Cancer Lett. 2024; 587:216701.
- Mao M, Chen W, Huang X, et al. Role of tRNA-derived small RNAs(tsR-NAs) in the diagnosis and treatment of malignant tumours. Cell Commun Signal. 2023;21(1):178.
- Xie Y, Yao L, Yu X, et al. Action mechanisms and research methods of tRNA-derived small RNAs. Signal Transduct Target Ther. 2020;5(1):109.
- China Clinical Oncology Society Guidelines Working Committee. China Clinical Oncology Society CSCO Nasopharyngeal Carcinoma Diagnosis and Treatment Guidelines 2024. Beijing: People's Medical Publishing House, 2024.08.
- Huang GF, Xiong D, Xie H. Discussion on the relationship between spleen deficiency and nasal spasm. Clinical Research of Traditional Chinese Medicine, 2014, 6 (23):34-35.
- Fang L, Guo H, Wang A J, et al. Discussion on TCM diagnosis and treatment of epistaxis based on "fire inflammation". Journal of Eye, Ear, Nose and Throat of Traditional Chinese Medicine, 2024, 14 (04):189-190+194.
- Liao Y, XIE H. Treatment of nasal congestion from heat based on the theory of "excess causes harm, inherited Nai system". China Folk Therapy, 2021, 29 (19):10-12.
- Xun MX, Zang JH, Jin WG. Clinical observation of Qingfei powder in treating perennial allergic rhinitis. Modern Distance Education of China Traditional Chinese Medicine, 2020, 18 (04):252-254.
- Sun QC, Han GQ, Shan H. Discussion on TCM differentiation and treatment of malignant tumor. Clinical Research of Traditional Chinese Medicine, 2016, 8 (08):63-64.
- Li YL, Zhou LP, Liu QL, et al. Malignant tumor treated from Qi. Clinical Journal of Traditional Chinese Medicine, 2022, 34 (03):399-403.

- Chen M X, Kang S Y, Zhao D, et al. Discussion on the prevention and treatment of depression by TCM compound prescription from TCM syndrome differentiation. Chinese Medicine New Drugs and Clinical Pharmacology, 2025, 36 (03):479-488.
- Yu Z, Huang XH, Teng JR, et al. The theoretical connotation and clinical application of liver governing the smooth flow of emotion. Journal of Traditional Chinese Medicine, 2013, 54 (22):1914-1916.
- Zhou Q, Zhang H, Chen MX. Treatment of malignant tumor from Qi theory of TCM. Journal of Clinical TCM, 2022, 34 (12):2245-2249.
 Li LZ. Clinical observation on the effect of invigorating spleen and nourish-
- 24. Li LZ. Clinical observation on the effect of invigorating spleen and nourishing liver method on the quality of life of patients with spleen deficiency and liver depression after radiotherapy and chemotherapy for nasopharyngeal carcinoma. Chengdu University of Traditional Chinese Medicine, 2018.
- Gao ZW, Zhou YČ, Guo JH, et al. Correlation between TCM syndromes and TGF-β1 in patients with nasopharyngeal carcinoma. Journal of Practical Internal Medicine of Traditional Chinese Medicine. 2015. 29 (08):1-2
- Peng ZW, Li J, Zeng BR. Effect of Xihuang Pill on quality of life of radiotherapy patients with nasopharyngeal carcinoma of fire toxin and blood stasis type. Journal of Anhui University of Traditional Chinese Medicine, 2017, 36 (06):17-20.
- Wang ZS, Wang XQ, Cheng FF, et al. A case of recurrent epistaxis in children treated with Qinggan Yinjing Decoction. Global Journal of Traditional Chinese Medicine, 2016, 9 (11):1403-1405.
- He DW, Shi FY, Gao SX, et al. Clinical observation on modified Xin 'an Biyuan recipe for epistaxis. Yunnan Journal of Traditional Chinese Medicine, 2023, 44 (01):58-61.
- Chen JX, Deng X. Curative effect observation on treating epistaxis by purging south and reinforcing north. Inner Mongolia Journal of Traditional Chinese Medicine, 2017, 36 (01):18-19.
 Liu S J, Tian D A, He Y J, et al. Correlation between TCM syndromes and
- Liu S J, Tian D A, He Y J, et al. Correlation between TCM syndromes and intracranial invasion potential of nasopharyngeal carcinoma. China Journal of Integrated Traditional Chinese and Western Medicine, 2006, (12):1086-1089.
- Qiu BS, Zhong TG, Wang SH, et al. Preliminary study on the relationship between TCM syndrome differentiation and histopathology of nasopharyngeal carcinoma. Journal of Guangzhou University of Traditional Chinese Medicine, 1998,(02):24-27.
- Wang XW, Jiang ZC, Tang FQ, et al. Theoretical basis and application of pathogenesis of "qi deficiency and poisoning" in nasopharyngeal carcinoma. China Journal of Integrated Traditional Chinese and Western Medicine. 2022. 30 (04):314-316-320
- cine, 2022, 30 (04):314-316+320.
 33. Yang W L, Wang X W, Li L, et al. Professor Tian F A's prescription strategy for treating nasopharyngeal carcinoma with deficiency of qi and yin after radiotherapy. Journal of Hunan University of Traditional Chinese Medicine, 2022, 42 (06):974-980.
- Ning CH, Peng QP, Tian GX, et al. Synergistic and Attenuating Effects of Modified Yiqi Yangyin Jiedu Recipe on Nasopharyngeal Carcinoma Patients with Qi-Yin Deficiency and Toxic Heat Accumulation in Lung after Radiotherapy and Chemotherapy. Journal of Hunan University of Traditional Chinese Medicine, 2025, 45 (01):158-163.
- Huang Y. Study on the evolution of TCM syndromes in patients with nasopharyngeal carcinoma treated with radiotherapy and chemotherapy based on cluster analysis. Inner Mongolia Journal of Traditional Chinese Medicine, 2023, 42 (05):146-148.
- Wang MY. Clinical observation on Jiawei Maimendong Decoction combined with cisplatin concurrent chemoradiotherapy for locally advanced nasopharyngeal carcinoma patients with deficiency of both Qi and Yin. Anhui University of Traditional Chinese Medicine, 2024.
- Liu SH, Peng J, Tang L B, et al. Effect of Bazhen Decoction and Wuwei Xiaoduyin on concurrent chemoradiotherapy and quality of life in patients with locally advanced nasopharyngeal carcinoma with deficiency of both qi and yin. China Journal of Clinicians, 2024, 52 (01):115-118.
- Yang YZ. Clinical observation of Yangyin Quyu Fang in treatment of qi-yin deficiency syndrome after radiotherapy and chemotherapy for nasopharyngeal carcinoma. Shiyong Zhongyi Zazhi, 2023, 39 (08):1541-1543.
- Zhou Q. Clinical observation of Jiawei Shengmai Powder combined with Nimotuzumab in the treatment of stage III/IV EGFR positive nasopharyngeal carcinoma patients with deficiency of both qi and yin. Hunan University of Traditional Chinese Medicine, 2023.
- Ma GH, Dong YL, Wu N, et al. Effect of Yangyin Jiedu Decoction on immune function and cancer-related fatigue in patients with advanced nasopharyngeal carcinoma treated with radiotherapy and chemotherapy. Shaanxi Journal of Traditional Chinese Medicine, 2022, 43 (10):1407-1410.
- Lu Z, Su K, Wang X, et al. Expression Profiles of tRNA-Derived Small RNAs and Their Potential Roles in Primary Nasopharyngeal Carcinoma. Front Mol Biosci. 2021;8:780621.
- Li H, Wang X, Sun A, et al. tRF-1:28-Val-CAC-2 promotes the development of nasopharyngeal cancer by targeting EPHB2. Front Oncol. 2025;15:1564601.

44 | Research article

Supplementary File 1 | Clinical data with baseline characteristics of NPC patients

Patient ID	Gender	Age	Histology	Pathological Grade	Pathological Stage	Ki-67	EBER
1	Male	49	Non-keratinous carcinoma, Differentiated type	T1N1M0	II	80%	+
2	Female	51	Non-keratinous carcinoma, Undifferentiated type	T2N3M1	IVb	60-70%	+
3	Male	37	Non-keratinous carcinoma, Undifferentiated type	T2N1M0	II	60%	+
4	Female	60	Non-keratinous carcinoma, Undifferentiated type	T2N3M0	IVa	40%	+
5	Male	46	Non-keratinous carcinoma, Undifferentiated type	T2N3M0	IVa	20%	+
6	Male	51	Non-keratinous carcinoma, Undifferentiated type	T4N3M0	IVa	50%	+
7	Male	56	Non-keratinous carcinoma	T3N3M1	IVb	50%	+
8	Male	32	Non-keratinous carcinoma, Undifferentiated type	T3N1M0	III	40-50%	+
9	Female	50	Non-keratinous carcinoma, Undifferentiated type	T2N1M0	II	50%	+
10	Male	42	Non-keratinous carcinoma, Undifferentiated type	T3N3M0	IVa	40%	+
11	Male	56	Non-keratinous carcinoma, Undifferentiated type	T4N1M0	IVa	30%	+
12	Male	52	Non-keratinous carcinoma, Undifferentiated type	T4N3M0	IVa	60%	+
13	Female	65	Non-keratinous carcinoma, Undifferentiated type	T2N2M0	III	50%	+
14	Female	65	Non-keratinous carcinoma, Undifferentiated type	T2N3M0	IVa	40%	+
15	Male	68	Moderately differentiated squamous cell	T2N0M0	II	80%	+
16	Male	61	Non-keratinous carcinoma, Undifferentiated type	T3N1M0	III	80%	+
17	Female	46	Non-keratinous carcinoma, Undifferentiated and differenti- ated mixed type	T3N2M0	III	30%	+
18	Male	41	Non-keratinous carcinoma, Undifferentiated type	T2N2M0	II	70%	+
19	Male	54	Non-keratinous carcinoma, Undifferentiated type	T4N2M0	IVa	80%	+
20	Male	57	Non-keratinous carcinoma, Undifferentiated type	T1N3M0	IVa	40%	+